The Meridional and Seasonal Structures of the Mixed-Layer Depth and its Diurnal Amplitude Observed during the Hawaii-to-Tahiti Shuttle Experiment*

NIKLAS SCHNEIDER AND PETER MÜLLER

Department of Oceanography and Hawaii Institute of Geophysics, University of Hawaii at Manoa, Honolulu, Hawaii

(Manuscript received 12 September 1989, in final form 20 February 1990)

ABSTRACT

We describe the meridional and seasonal structures of daily mean mixed-layer depth and its diurnal amplitude and their relation to atmospheric fluxes by compositing mixed-layer depth estimates derived from density observations. The diurnal mean mixed-layer depth shows a ridge at the equator, troughs, which vary seasonally in intensity, at 10° to 15°N and 5° to 10°S, and a trough appearing just north of the equator in the second half of the year. This is in contrast to the ridge–trough structure of the top of the main thermocline, which reflects the dynamic topography associated with the equatorial current system. The diurnal amplitude is significantly different from zero for most latitudes year-round, indicating that the diurnal cycle of mixed-layer depth is a widespread phenomenon. For sufficiently strong heating, both the mixed-layer depth and its diurnal amplitude are significantly correlated with Monin-Obukhov length scales based on the mean net heat flux, mean wind stress, and mean shortwave radiation. This suggests a possible parameterization of the mixed-layer depth and diurnal amplitude in terms of the mean atmospheric fluxes for meridional scales of a few degrees and seasonal time scales.

1. Introduction

The thickness of the surface mixed layer determines both the thermal and the mechanical inertia of the layer in direct contact with the atmosphere and influences the fluxes at the base of the layer. Hence the mixed-layer depth will affect the oceanic response to the prescribed surface forcing and the evolution of the coupled ocean–atmosphere system. Thus, the study of mixed-layer depth and its variability is of great importance for the understanding and interpretation of thermal and velocity fields of the upper ocean, for parameterizing mixed-layer processes, and for air–sea interaction.

In the central equatorial Pacific the depth of the mixed layer was traditionally associated with the top of the main thermocline and described as such (e.g., Wyrtki 1964). However, an inspection of individual temperature, salinity or density profiles reveals that mixed layers are usually much shallower than the top of the themocline. Therefore, it becomes necessary to describe the unknown seasonal and meridional structures of the thickness of this layer.

Additionally, observations obtained during the 1984 Tropic Heat experiment at 140°W on the equator showed a strong diurnal signal of the mixed-layer depth (Gregg et al. 1985; Peters et al. 1989: Moum et al. 1989). However, a description of the longer-term and larger-scale variability of daily mean mixed-layer depth and its diurnal signal was not possible because of the short duration and limited spacial extent of this experiment.

We use the extended time and large meridional coverage of the Hawaii-to-Tahiti Shuttle experiment to describe the seasonal and meridional structures of the mixed-layer depth and its diurnal amplitude and to investigate their relation to atmospheric fluxes. A brief description of the experiment follows and the estimation of the mixed-layer depth from density observations is discussed. Because we find a diurnal cycle in the mixed-layer depth estimates we are able to extract the diurnal mean mixed-layer depth and the diurnal amplitude from the data. We show their seasonal and meridional structures and find that the mixed-layer depth and top of the main thermocline have very different structures and that the diurnal cycle of mixed-layer depth is a widespread phenomenon. Finally we discuss the correlations of the diurnal mean mixed-layer depth and the diurnal amplitude with observed atmospheric forcing and introduce possible parameterizations of mixed-layer depth and diurnal amplitude in terms of the Monin-Obukhov depth.

2. Data

The Hawaii-to-Tahiti Shuttle experiment took place during 17 months from 1979 to 1980 and is described

* Hawaii Institute of Geophysics Contribution Number 2311.

Corresponding author address: N. Schneider, 1000 Pope Road, Honolulu, Hawaii 96822.

in detail by Wyrtki et al. (1981). Starting in February 1979, 15 approximately monthly cruises were undertaken along three transects: 158°W, 153°W and 150°W. Fourteen of these spanned the distance between Hawaii (21°N) and Tahiti (17°S), typically following the cruise track given in Fig. 1. Among other observations, CTD casts were taken from the surface to approximately 1000 m at every full degree of latitude or longitude. A total of 1125 stations were occupied. The processed records (Williams 1981) give depth, temperature, potential temperature, salinity, density σ_T, and potential density σ_θ, all as a function of pressure with a vertical resolution of 2.5 db.

The components of heat flux and wind stress were obtained from meteorological observations performed several times each day (Stevenson 1982). The bulk formulas used did not resolve the diurnal signal of the incoming shortwave radiation. Instead its daily mean value was obtained. Lukas and Firing (1985) discussed the representativeness of the Hawaii-to-Tahiti Shuttle data and concluded that the experiment took place during normal or near normal wind conditions for the central Pacific.

3. Mixed layer criteria

Several different approaches have been followed in estimating mixed-layer depth from observations of the structure of the upper ocean. Gradients or differences from the surface of either temperature, salinity or density are specified which cannot be exceeded within the mixed layer. Wyrtki (1964) used a temperature difference of 0.5°C. Lukas and Lindstrom (1987) employed critical gradients of temperature (0.05°C m^{-1}, 0.025°C m^{-1}), salinity (0.02 m^{-1}, 0.01 m^{-1}), and potential density σ_θ (0.01 kg m^{-4}). Peters et al. (1989) used a difference of σ_θ of 0.01 kg m^{-3}.

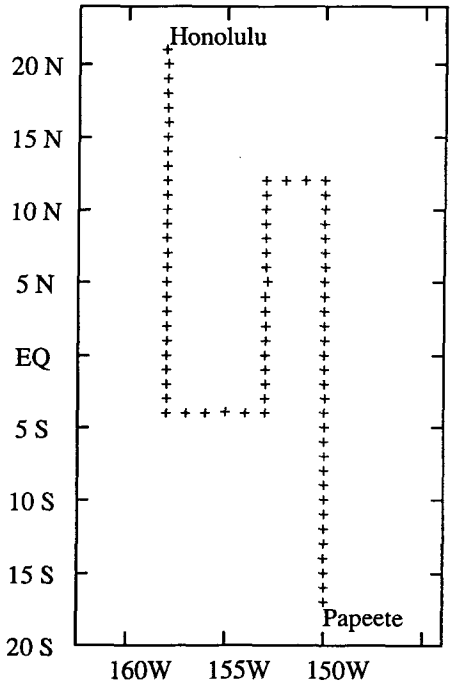

FIG. 1. Typical cruise track and station distribution of the Hawaii-to-Tahiti Shuttle experiment.

In general the estimation of the mixed-layer depth from density should involve potential density σ_θ or σ_T instead of *in situ* density because the vertical overturning by turbulence can cause an adiabatic in situ density change of 0.04 kg m^{-3} over a vertical distance of 10 m. This is mainly due to the compressibility of sea water.

For this dataset we find that Lukas and Lindstroms' (1987) density gradient criterion is not a consistent estimator of the mixed-layer depth, but often detects the top of the main thermocline. However, mixed-layer depth estimates based on a density difference of 0.01 kg m^{-3} coincides approximately with subjective estimates of the mixed-layer depth. Therefore, we define the mixed-layer depth as the deepest level where potential density σ_θ does not exceed surface density by more than 0.01 kg m^{-3}, thus employing the same criterion as Peters et al. (1989). To investigate sensitivity to changes of the criterion, we compare the mixed-layer depth estimates with those based on a density difference of 0.03 kg m^{-3}. Because density observations at 0 db are unreliable, the surface value is taken at 2.5 db.

It should be noted that a difference criterion does not recognize a newly formed (e.g., diurnal) mixed layer before the surface buoyancy flux changes the mixed-layer density sufficiently. The resulting phase lag of the estimated mixed-layer response increases for larger density criteria.

4. Definition of diurnal mean mixed-layer depth and diurnal amplitude

Formation of a composite daily cycle from all mixed-layer depth estimates yields a strong diurnal signal (Fig. 2). The mixed layer is deepest in the early morning, becomes rapidly shallower after 0900 LST and reaches minimum values during the afternoon. After sunset, the mixed layer deepens again until the early morning. The difference between the depth minimum and maximum is 31 m, about 11 times larger than the typical error of the mean (2.75 m). This surprisingly strong diurnal signal enables us to extract from the data the diurnal mean mixed-layer depth $\bar{h}$ and the diurnal amplitude A of the mixed-layer depth.

We define the amplitude A as the difference of the mean night (2000 to 1000 LST) mixed-layer depth and the mean day (1000 to 2000 LST) mixed-layer depth. For the composite the mean amplitude is 20 m (Fig. 2). Its variance is estimated as the sum of the variances of mean day and mean night mixed-layer depths.

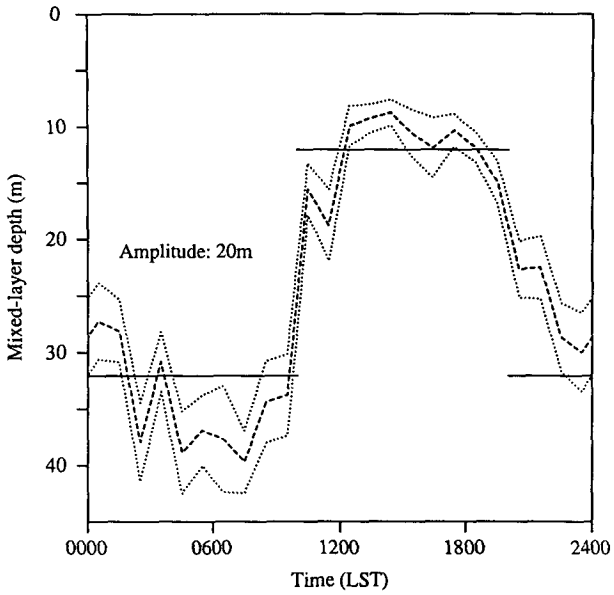

FIG. 2. Composite diurnal cycle of mixed-layer depth formed by averaging all data within one hour bins. The dashed line depicts the hourly mean depth, the dotted shows one standard error of the mean. The solid lines show the mean night (2000 to 1000 LST) and mean day (1000 to 2000 LST) mixed-layer depths. The difference between these two defines the diurnal amplitude.

In calculating the diurnal mean mixed-layer depth $\bar{h}$, care must be taken to avoid biases due to the combination of the diurnal signal and different numbers of observations during day and night. Therefore, the diurnal signal is removed prior to the calculation of $\bar{h}$ and its variance by subtracting $^{10}/_{24}$ of the amplitude from night observations and by adding $^{14}/_{24}$ of the amplitude to day observations. For the composite the daily mean mixed-layer depth is 24 m.

These procedures are equivalent to least-square fitting a highly simplified model for the diurnal variation of the mixed-layer depth h to the data, i.e.,

$$h = \begin{cases} \bar{h} - \frac{14}{24}A & \text{from 1000 to 2000 LST} \\ \bar{h} + \frac{10}{24}A & \text{from 2000 to 1000 LST.} \end{cases}$$

To obtain the meridional and seasonal structures of $\bar{h}$ and A for a typical longitude of the Hawaii-to-Tahiti Shuttle experiment, we project all data into one year, disregard zonal differences, and form bins as shown in Fig. 3. Because of the inhomogeneous data distribution the limits of the bins were chosen to combine adjacent data points and to contain a minimum of eight observations. From 4.5°S and 12.5°N poleward the data density permits averaging over 2.4 months and 4° to 7° of latitude. Between 4.5°S and 12.5°N the meridional resolution of the averaging procedure is increased to 3° to 4° of latitude and 2 months.

For each bin a composite diurnal cycle of mixed-layer depth is formed by stratifying the data into day and night observations. Then the average diurnal amplitude $\langle A \rangle$, the average diurnal mean mixed-layer depth $\langle \bar{h} \rangle$, and their respective standard errors are obtained. Assuming that all observations in a bin are in-

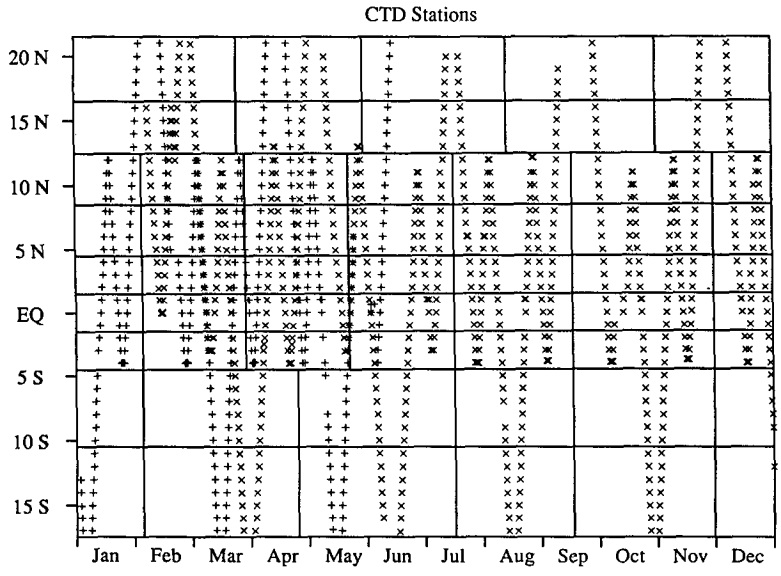

FIG. 3. Seasonal and meridional distribution of mixed-layer depth estimates. Fifteen months of data from 1979 (denoted by ×) and 1980 (denoted by +) were projected into one model year. Zonal and interannual variations were disregarded. The solid lines show the bins over which the mixed-layer depth estimates were averaged. South of 13°N data from December and January were binned together.

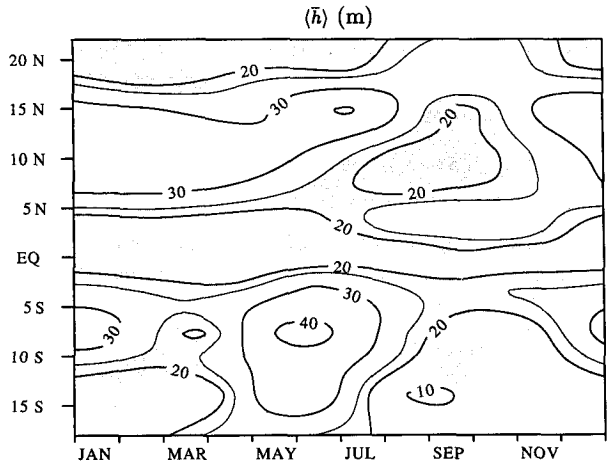

FIG. 4. Seasonal and meridional dependence of the mixed-layer depth $\langle \bar{h} \rangle$ in meters. Mixed-layer depths smaller than the average mixed-layer depth (24 m) are shaded.

dependent, and that the estimates for the mean mixed-layer depth and mean diurnal amplitude are normally distributed around their true values, we are able to compute confidence intervals.

5. Results

We present the meridional and seasonal structures of the mixed-layer depth and diurnal amplitude as contour plots and as meridional and seasonal sections with confidence intervals. While the contour plots are best suited to see overall variability and absolute levels, the sections give an impression of the significance of the results. Because the limits of the bins depend on latitude, data from two-month periods are displayed together.

a. Diurnal mean mixed-layer depth

For most of the year, the mixed-layer depth $\langle \bar{h} \rangle$ shows a ridge at the equator and troughs at 10° to 15°N and, less developed, at 5° to 10°S (Figs. 4 and 5). While the depth of the equatorial ridge remains constant at 15 m throughout the year, the troughs undergo strong seasonal variations (Fig. 6). In the Northern Hemisphere the trough exceeds a depth of 35 m during the first half of the year and disappears during August through November by becoming as shallow (19 m) as the equatorial ridge. During this time a weak local trough develops at 3°N narrowing the equatorial ridge. Thus the phase of the seasonal signal at this latitude is shifted by about half a year compared to farther north. In the Southern Hemisphere a strong trough of mixed-layer depth develops during the southern winter with depths deeper than 40 m. During the rest of the year the Southern Hemisphere trough is weak or nonexistent. We do not consider the deep mixed-layer depth observations at 8°S in December and January to be significantly different from the surrounding observations.

Especially in the equatorial region, this structure is very different from the depth of the top of the thermocline (Fig. 7). The top of the thermocline has a distribution of ridges and troughs typical for the meridional structure of the main thermocline and dynamic height in the central Pacific (Wyrtki and Kilonsky 1984). In the Northern Hemisphere the boundaries of the Equatorial Counter Current are marked by a deep thermocline at about 3°N and shallow ones at 10°N. The equator shows a bulging thermocline from March to July. In the Southern Hemisphere the trough of the top of the main thermocline at 5°S is deepest from August to February. This description is consistent with the findings of Wyrtki (1964), for the regions to the east of 140°W.

b. Diurnal amplitude of mixed-layer depth

For the calculation of the diurnal amplitude $\langle A \rangle$ the mixed-layer depth estimates in each bin are sorted with respect to day or night. Therefore the number of degrees of freedom is reduced and the confidence intervals are approximately doubled compared to the results for $\langle \bar{h} \rangle$.

The estimates of the diurnal amplitude indicate that the diurnal cycle of the mixed-layer depth is a widespread phenomenon. At almost all latitudes and times

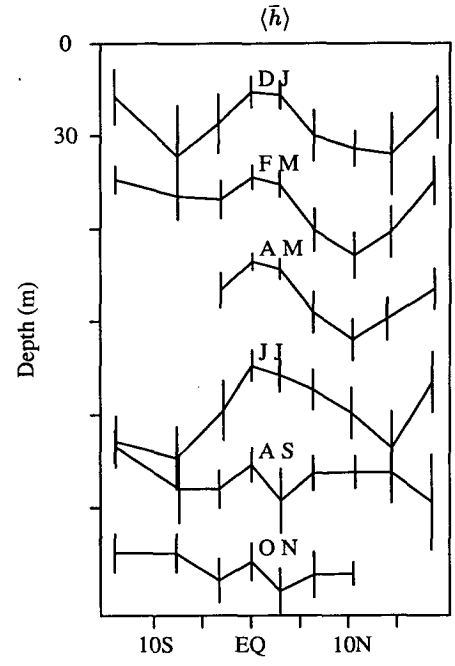

FIG. 5. Stack plot of meridional sections of mixed-layer depth $\langle \bar{h} \rangle$ in meters. Offset between consecutive sections is 30 m. Data from indicated two-month periods (indicated by first letters of months) are displayed together. The error bars denote the 95% confidence intervals.

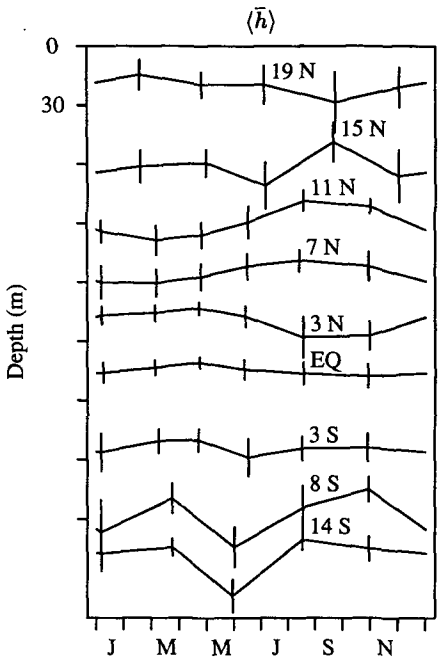

FIG. 6. Stack plot of seasonal sections of mixed-layer depth $\langle \bar{h} \rangle$ in meters. The offset between consecutive sections is 30 m. Labels at the abscissa denote every second month. The mean latitude of the data is indicated. The error bars show the 95% confidence intervals.

the diurnal amplitude is significantly different from zero (Fig. 8).

The meridional sections reveal that the main variability of the diurnal amplitude is in a meridional direction (Fig. 9). For most of the year, the diurnal amplitude exhibits a ridge–trough structure similar to that of the mixed-layer depth. Two maxima of the amplitude at 10° to 15°N and at 2° to 10°S are observed from December to June (Figs. 8 and 9). In the remaining months the northern hemisphere maxima appear just north of the equator between 2° and 5°N.

A seasonal cycle of $\langle A \rangle$ (Fig. 10) can be detected in the latitude band just north of the equator (1° to 5°N). There the diurnal amplitude changes from about 15 m in December through April to about 40 m in August. For the remaining latitudes (11°N, 7°N, equator and 8°S), the diurnal amplitude is either approximately constant, or (19°N, 15°N, 3°S and 14°S) more variable without a discernible significant seasonal signal.

c. *Sensitivity*

The sensitivity of the results is investigated by recalculating the diurnal mean mixed-layer depth and the diurnal amplitude using a mixed-layer density criterion of 0.03 kg m^{-3}. In the following the criterion used is indicated by a subscript. For example, $\langle \bar{h} \rangle_{0.03}$ indicates the diurnal mean mixed-layer depth based on a density difference of 0.03 kg m^{-3}.

The correlation of $\langle \bar{h} \rangle_{0.01}$ and $\langle \bar{h} \rangle_{0.03}$ is 0.95 with a 95% significance level of 0.29. On the average the larger density criterion increases the mixed-layer estimates by ten meters. This indicates a mean vertical density slope of 2×10^{-3} kg m^{-4} in the depth range beneath $\langle \bar{h} \rangle_{0.01}$. The difference is largest in the Southern Hemisphere between 5° and 10°S where it varies between 10 and 20 m in phase with the seasonal cycle. In the Northern Hemisphere the largest differences occur between 5° and 15°N in the first half of the year and the smallest differences occur during the second half. Thus the seasonal cycle of the mixed-layer depth in these latitude bands is enhanced by approximately 10 m for the 0.03 kg m^{-3} criterion but not qualitatively changed.

Overall, the absolute value of the mixed-layer depth is sensitive to the mixed-layer criterion, and should be treated with caution. However, its meridional and seasonal dependencies are robust results. Peters et al. (1989) concluded similarly that the variability pattern of the mixed-layer depth is not changed by using different values for the density criterion.

The correlation of the diurnal amplitudes $\langle A \rangle_{0.03}$ and $\langle A \rangle_{0.01}$ is 0.79 (95% significance level: 0.29). The meridional and seasonal dependence of the difference $\langle A \rangle_{0.03} - \langle A \rangle_{0.01}$ has no systematic bias but shows both positive and negative values (Fig. 11). The largest positive differences occur in the Southern Hemisphere from August to November. Large negative differences are found in the Northern Hemisphere from December to April, at 20°N in August and in the Southern Hemisphere at 15°S in May and June. However, the overall shape of the seasonal and meridional variations are not changed.

Incidentally, the sign of $\langle A \rangle_{0.03} - \langle A \rangle_{0.01}$ indicates the average steepness of density profiles beneath the mixed layer. The mixed-layer depth estimate based on

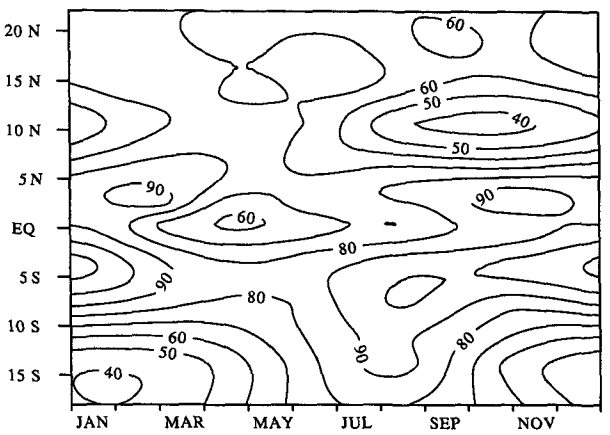

FIG. 7. Seasonal and meridional dependence of the top of the main thermocline in meters, estimated as the deepest level where the surface density is not exceeded by more than 0.3 kg m^{-3}. Values shallower than 70 m are shaded.

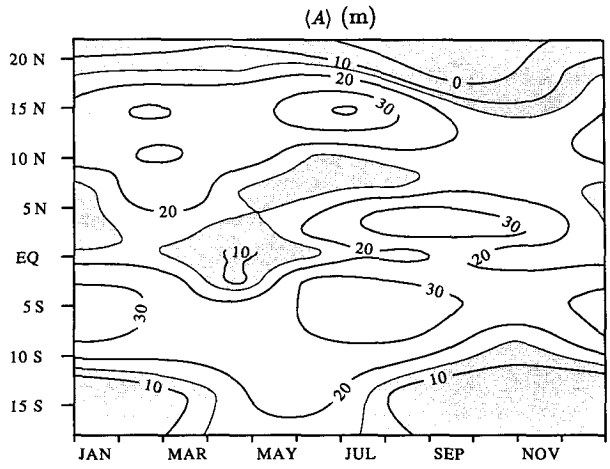

FIG. 8. Seasonal and meridional structure of diurnal amplitude $\langle A \rangle$ of mixed-layer depth in meters. The diurnal amplitude is defined as the difference of mean night (2000 to 1000 LST) and mean day (1000 to 2000 LST) mixed-layer depth. Diurnal amplitudes smaller than the typical 95% confidence limit (14 m) are shaded.

the density criterion of 0.03 kg m^{-3} is either equal to or larger than the depth estimated using a smaller criterion. Therefore a positive value of $\langle A \rangle_{0.03} - \langle A \rangle_{0.01}$ indicates that the difference of night mixed-layer estimates is larger than the difference of day estimates while a negative value implies the opposite. If the base of the mixed layer is marked by a very strong density gradient, both density criteria yield similar results. For a weak gradient the estimates are farther apart. Thus the areas of positive values $\langle A \rangle_{0.03} - \langle A \rangle_{0.01}$ can be characterized by poorly marked bases of the night mixed layer. For latitudes and months with negative values $\langle A \rangle_{0.03} - \langle A \rangle_{0.01}$ the day mixed layer is not strongly developed and the larger mixed-layer density criterion misses shallow diurnal mixed layers. This intepretation is supported by an inspection of individual profiles.

6. Atmospheric fluxes

Because the mixed layer is strongly influenced by atmospheric forcing, we now describe relevant forcing fields and investigate their relation to the mixed-layer depth and diurnal amplitude estimates in the following section. Stevenson and Niiler (1983) presented all components of the heat flux observed during the Hawaii-to-Tahiti Shuttle experiment in latitude bands as deviations from the 15-cruise mean. We obtained the seasonal and meridional structures of the mean net daily heat flux $\langle \bar{Q} \rangle$, the mean daily shortwave heat flux $\langle \bar{Q}_{sw} \rangle$, and the mean wind stress magnitude $\langle \tau \rangle$ by averaging over the same time and meridional bins as the mixed-layer depth (see Fig. 3), thus focusing on the seasonal and meridional structures.

Poleward of 5°N and 5°S the incoming shortwave radiation $\langle \bar{Q}_{sw} \rangle$ has maximum values in summer and minimum values in winter (Fig. 12). In the equatorial band biannual variations can be seen with minima in June and December and maxima around the time of equinox. Away from the equator the seasonal variation is mainly due to the position of the sun, while in the lower latitudes it is caused by the seasonal variation of cloudiness (Stevenson and Niiler 1983).

The magnitude of the wind stress $\langle \tau \rangle$ shows the seasonal variability of the trade wind field (Fig. 13). The northeast trades reach farthest equatorward and are strongest in northern winter. In the Southern Hemisphere the seasonal signal is not as pronounced. Wind stress is smallest during southern summer. The equator displays weakest winds during April, June and July.

The net heat flux $\langle \bar{Q} \rangle$ shows a strong seasonality in both hemispheres with largest heating during summer and cooling in winter (Fig. 14). The equatorial region shows strongest heating during February to May. In general, the area experiences positive heat fluxes for most of the year.

7. Atmospheric forcing

We now consider the relation of the mixed-layer depth and diurnal amplitude with the atmospheric fields. Considering first the mixed-layer depth, we find that its correlation with the net heat flux $\langle \bar{Q} \rangle$ is negative and with the wind stress $\langle \tau \rangle$ is positive (Table 1). This indicates that in general the mixed layer is deeper for small heat fluxes and strong wind stresses.

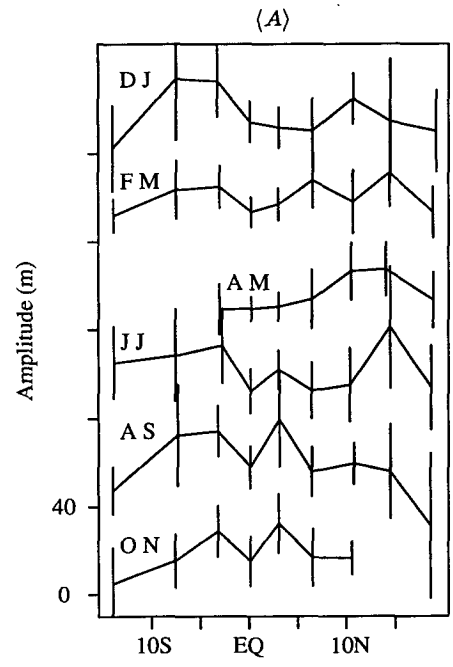

FIG. 9. Stack plot of meridional sections of the diurnal amplitude of mixed-layer depth. Offset between consecutive sections is 40 m. Data from indicated two-month periods (indicated by first letters of months) are displayed together. The error bars denote the 95% confidence intervals.

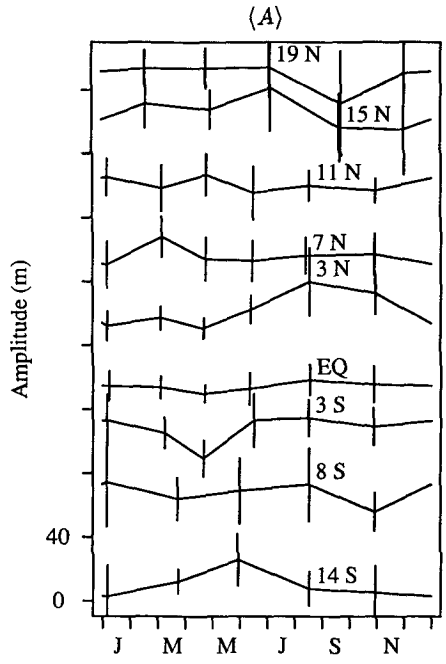

FIG. 10. Stack plot of seasonal sections of the diurnal amplitude $\langle A \rangle$ of the mixed-layer depth. Labels at the abscissa denote every second month. The offset between consecutive sections is 40 m. The mean latitude of the data is indicated. The error bars show the 95% confidence intervals.

The combined effect of the surface heat flux and the wind stress on the mixed-layer depth is described by the Monin-Obukhov depth L

$$L = 2\left(\frac{\tau}{\rho_0}\right)^{3/2}\left(\frac{\alpha g}{\rho_0 c_p} Q\right)^{-1}$$

where ρ_0 is a reference density, α the thermal expansion coefficient, c_p the specific heat, and g the gravitational acceleration. The length scale L describes the depth of a layer for which the increase of the potential energy by downward mixing of the surface buoyancy flux is balanced by the flux of turbulent kinetic energy supplied by the wind. This balance can be achieved only for sufficiently positive buoyancy fluxes, corresponding to heating or rain. For weak heating or cooling situations other terms of the turbulent kinetic energy equation (e.g., dissipation) become important, and the Monin-Obukhov depth is not the relevant depth scale.

We estimate the averaged Monin-Obukhov depth $\langle \bar{L} \rangle$ from the averaged heat flux $\langle \bar{Q} \rangle$ and wind stress $\langle \tau \rangle$, thereby neglecting the effect of synoptic fluctuations. Thus we have

$$\langle \bar{L} \rangle = 2\left(\frac{\langle \tau \rangle}{\rho_0}\right)^{3/2}\left(\frac{\alpha g}{\rho_0 c_p} \langle \bar{Q} \rangle\right)^{-1}.$$

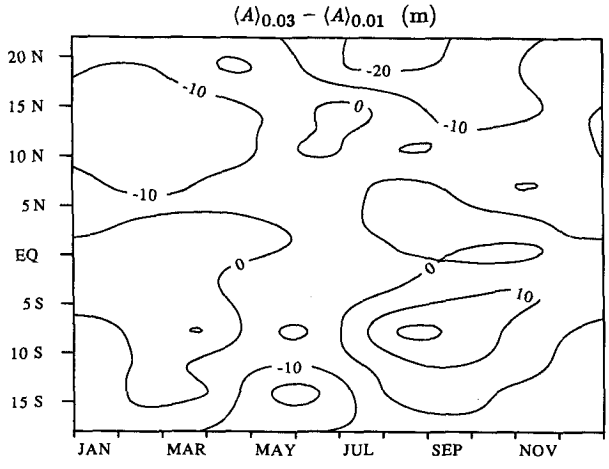

FIG. 11. Difference of diurnal amplitudes of mixed-layer depth based on density differences of 0.03 and 0.01 kg m^{-3}.

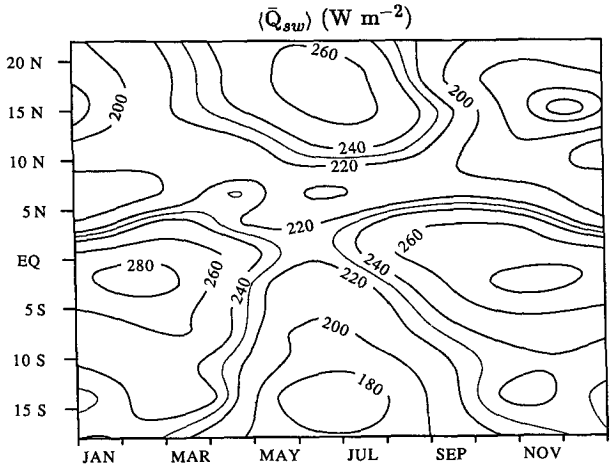

FIG. 12. Seasonal and meridional structure of averaged short wave radiation $\langle \bar{Q}_{sw} \rangle$ in W m^{-2}. Values smaller than 230 W m^{-2} are shaded.

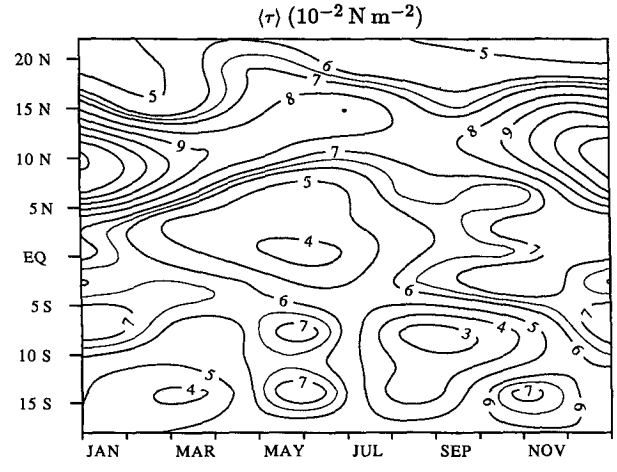

FIG. 13. Seasonal and meridional structure of averaged wind stress $\langle \tau \rangle$ in 10^{-2} N m^{-2}. Values smaller than 6.5×10^{-2} N m^{-2} are shaded.

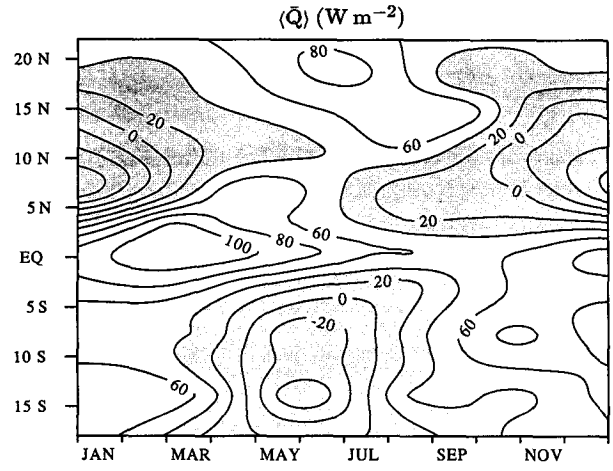

FIG. 14. Seasonal and meridional structure of averaged net heat flux $\langle \bar{Q} \rangle$ in W m^{-2}. Values smaller than 40 W m^{-2} are shaded.

Taking into consideration only data points corresponding to a heat flux $\langle \bar{Q} \rangle$ of more than 20 W m^{-2}, the mixed-layer depth $\langle \bar{h} \rangle$ and Monin-Obukhov depth $\langle \bar{L} \rangle$ are significantly correlated (correlation coefficient: 0.70) to the 95% significance level (0.33) (Fig. 15). The linear regression (with 95% confidence interval) is given by

$$\langle \bar{h} \rangle = (13.2 \text{ m} \pm 3.3 \text{ m}) + (0.31 \pm 0.11)\langle \bar{L} \rangle.$$

Again, the zero crossing indicates that the mixed-layer criterion used overestimates the mean mixed-layer depth obtained from this fit.

This correlation and regression suggest a possible parameterization of the mixed-layer depth $\langle \bar{h} \rangle$ in terms of averaged heat flux $\langle \bar{Q} \rangle$ and wind stress $\langle \tau \rangle$.

Looking now at the relation of the diurnal amplitude $\langle A \rangle$ to atmospheric fields, we find that their correlations are very sensitive to the mixed-layer criterion. While $\langle A \rangle_{0.03}$ is significantly correlated only with the incoming shortwave heat flux $\langle \bar{Q}_{sw} \rangle$, amplitudes $\langle A \rangle_{0.01}$ are not significantly correlated with the incoming short wave heat flux (Table 1). However, their correlation with the mean mixed-layer depth is significant.

In the previous paragraph we showed that Monin-Obukhov scaling of the mixed layer depth is successful for sufficiently strong heating regimes. We therefore derive a scale for the diurnal amplitude based on Monin-Obukhov depth.

The diurnal cycle of mixed-layer depth is presumably caused by the diurnal cycle of shortwave radiation alone because the wind stress does not show a significant diurnal variation. Thus, the heat flux Q consists of a daily mean contribution $\bar{Q}$ and a diurnal signal δQ

$$Q = \bar{Q} + \delta Q.$$

The response of the Monin-Obukhov depth is then

$$\bar{L} - \delta L = \bar{L}\left(1 + \frac{\delta Q}{\bar{Q}}\right)^{-1}.$$

Therefore the scale δL of the diurnal amplitude of the mixed-layer depth is given by the difference of the diurnal mean value of the Monin-Obukhov depth $\bar{L}$ and its diurnal minimum.

Because our data do not resolve the diurnal cycle δQ, we estimate its magnitude by twice the daily mean shortwave radiation $\langle \bar{Q}_{sw} \rangle$. This is a good approximation in the tropics where the mean shortwave heat flux is mainly determined by its maximum amplitude; the variation of the length of day is less important.

We estimate the mean amplitude scale $\langle \delta L \rangle$ from the mean atmospheric observations, again neglecting the effect of synoptic fluctuations

$$\langle \delta L \rangle = \langle \bar{L} \rangle \left[1 - \left(1 + \frac{2\langle \bar{Q}_{sw} \rangle}{\langle \bar{Q} \rangle}\right)^{-1}\right].$$

Comparison of Figs. 12 and 14 shows that in general $\langle \bar{Q}_{sw} \rangle$ is much larger than $\langle \bar{Q} \rangle$. Therefore the second term on the right hand side is small compared to one, and the diurnal amplitude is mainly determined by the Monin-Obukov depth. This is consistent with the significant correlation of $\langle A \rangle$ and $\langle \bar{h} \rangle$ shown in Table 1.

The correlation of diurnal amplitude $\langle A \rangle$ with the Monin-Obukhov amplitude scale $\langle \delta L \rangle$ is significant if only values are taken into consideration which correspond to a net heat flux of more than 37 W m^{-2} (Fig. 16). The correlation coefficient is 0.54 with a 95% significance level of 0.39. The linear regression (with 95% confidence interval) for these values is

$$\langle A \rangle = (9.4 \text{ m} \pm 5.8 \text{ m}) + (0.43 \pm 0.27)\langle \delta L \rangle.$$

This correlation indicates a possible parameterization of the diurnal amplitude in terms of the mean atmospheric fluxes.

The correlation is very sensitive to the choice of mixed-layer criteria. For the diurnal amplitude based on a density difference of 0.03 kg m^{-3} the correlation (0.27) is not significant to the 95% significance level.

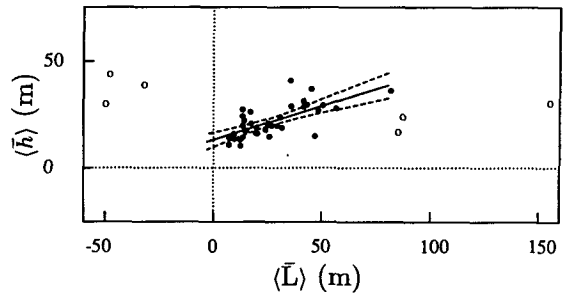

FIG. 15. Scatter plot of the Monin-Obukhov depth $\langle \bar{L} \rangle$ versus the mixed-layer depth $\langle \bar{h} \rangle$. The solid dots mark points associated with a net heat flux $\langle \bar{Q} \rangle$ of more than 20 W m^{-2}. Their correlation is 0.70 with a 95% significance level of 0.33. The linear regression (with 95% confidence interval) is

$$\langle \bar{h} \rangle = (13.2 \text{ m} \pm 3.3 \text{ m}) + (0.31 \pm 0.11)\langle \bar{L} \rangle$$

counting only the solid circles.

8. Conclusion and discussion

Data obtained during the Hawaii-to-Tahiti Shuttle experiment are used to describe the seasonal and meridional variation of diurnal mean mixed-layer depth and its diurnal amplitude. A density difference of 0.01 kg m^{-3} determined the mixed-layer depth from potential density observations. Although the Hawaii-to-Tahiti Shuttle was not designed as a mixed-layer study, the following results are obtained by compositing. For most of the year, mixed-layer depth shows a ridge at the equator and troughs at 10° to 15°N and at 5° to 10°S. While the depth of the equatorial ridge remains constant throughout the year, the depth of the troughs varies seasonally. In the second half of the year, a local trough develops just north of the equator. Overall, the mixed-layer depth is very different from the depth of the top of the thermocline.

For most latitudes and times diurnal amplitudes of the mixed-layer depth are significantly different from zero, indicating that the diurnal cycle of the mixed-layer depth is a widespread phenomenon. The main variability of the diurnal amplitudes is in meridional direction; in general the diurnal amplitude has a similar ridge–trough structure to the mixed-layer depth. Just north of the equator, diurnal amplitudes are largest in the second half of the year, showing the only significant seasonal variability. For the remaining latitudes, diurnal amplitudes are either constant or more variable without a discernible seasonal signal.

These findings are consistent with those obtained during the Tropic Heat experiment (Peters et al. 1989; Moum et al. 1989). In November of 1984 Peters et al. (1989) observed on the equator at 140°W a strong diurnal signal of mixed-layer depth. Between 1°S and 1.5°N mixed-layer depths were less than 10 m during the day and extended to 40 m at night. At 1°S and 1.5°N night values of the mixed-layer depth were as large as 60 m and 75 m, respectively. Mean depths were of the order of 25 m, slightly deeper than our estimates for the equator in November. From a time series on the equator obtained at the same time, Peters et al. (1989) estimated mean depth of approximately 20 m. The difference between day and night mixed-layer depth was of the order of 15 m. Moum et al. (1989) described a 12-day time series taken at the same time as Peters et al. (1989) at 140°W on the equator. They reported also a strong diurnal signal of mixed-layer depth. The depth varied from 10 m during day to 35 m during night. Considering that these are the extreme values of mixed-layer during the course of a day, and our estimates give an average difference of day and night mixed-layer depth, we see that our amplitude for November on the equator is in good agreement with their observations.

TABLE 1. Correlation of mixed-layer depth $\langle \bar{h} \rangle$ and the diurnal amplitude $\langle A \rangle$ based on a density difference of 0.01 and 0.03 kg m^{-3} (denoted by subscript) with the wind stress $\langle \tau \rangle$, net heat flux $\langle \bar{Q} \rangle$, daily averaged shortwave radiation $\langle \bar{Q}_{sw} \rangle$ and mixed-layer depth estimates. Fifty mean values were used to calculate the correlation coefficients. The 95% significance level is 0.29. Underlined values are referred to in the text.

	$\langle \tau \rangle$	$\langle \bar{Q} \rangle$	$\langle \bar{Q}_{sw} \rangle$	$\langle \bar{h} \rangle_{0.01}$	$\langle \bar{h} \rangle_{0.03}$
$\langle \bar{h} \rangle_{0.01}$	<u>0.61</u>	<u>−0.61</u>	−0.31	1	0.95
$\langle \bar{h} \rangle_{0.03}$	0.52	−0.58	−0.28	<u>0.95</u>	1
$\langle A \rangle_{0.01}$	0.21	−0.16	0.25	<u>0.54</u>	0.58
$\langle A \rangle_{0.03}$	−0.08	0.14	<u>0.50</u>	0.11	0.18

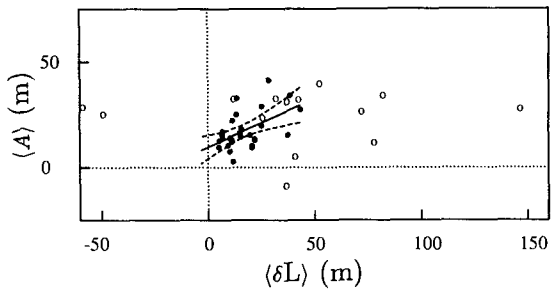

FIG. 16. Scatter plot of the Monin-Obukhov amplitude scale $\langle \delta L \rangle$ versus the diurnal amplitude estimates $\langle A \rangle$. The solid dots mark points associated with a net heat flux $\langle \bar{Q} \rangle$ of more than 37 W m^{-2}. Their correlation is 0.54 with a 95% significance level of 0.39. The linear regression (with 95% confidence interval) for these values is $\langle A \rangle = (9.4 \text{ m} + 5.8 \text{ m}) + (0.43 + 0.27) \langle \delta L \rangle$.

Our description of the diurnal amplitude of mixed-layer depth complements the study of Imawaki et al. (1988). They investigated the diurnal cycle of temperature of the upper equatorial ocean. Using time series of the temperature obtained at and to the east of 140°W, they showed a diurnal signal of sea surface temperature of the order of 0.1° to 0.3°K. This signal was confined to the upper 25 m of the water column throughout the year. Further to the east a seasonal signal of the penetration depth was found. We were not able to find a significant diurnal signal in the sea surface temperature data. This is presumably due to the masking of the diurnal signal by horizontal and other temporal inhomogeneities during compositing.

Beyond the description of the mixed-layer depth a second important outcome of our study is the significant correlations of the mixed-layer depths and the diurnal amplitudes with Monin-Obukhov scales neglecting synoptic fluctuations. These suggest a possible parameterization of the mixed-layer depth and its diurnal amplitude for seasonal time scales and meridional scales of a few degrees in terms of the mean atmospheric fluxes, i.e., from readily available charts of the monthly mean net heat flux, wind stress, and mean shortwave radiation.

Acknowledgments. This work was supported by National Science Foundation Grant OCE-85-15415. We thank Ren-Chieh Lien for helpful discussions and editorial assistance. Sharon Lukas provided expert com-

putational support. The efforts of Crystal Miles and Diane Henderson in improving the readability of this manuscript are gratefully acknowledged. We appreciate the thoughtful comments of two anonymous reviewers which greatly improved an earlier version of this manuscript.

REFERENCES

Gregg, M. C., H. Peters, J. C. Wesson, N. S. Oakey and T. J. Shay, 1985: Intensive measurements of turbulence and shear in the equatorial undercurrent. *Nature,* **318,** 140–144.

Imawaki, S., P. P. Niiler, C. H. Gautier, D. Halpern, R. A. Knox, W. G. Large, D. S. Luther, J. C. McWilliams, J. N. Moum and C. A. Paulson, 1988: A new method for estimating the turbulent heat flux at the bottom of the daily mixed layer. *J. Geophys. Res.,* **93,** 14 005–14 012.

Lukas, R., and E. Firing, 1985: The annual Rossby wave in the central equatorial Pacific ocean. *J. Phys. Oceanogr.,* **15,** 55–67.

——, and E. Lindstrom, 1987: The mixed layer of the western equatorial Pacific Ocean. *Dynamics of the Oceanic Surface Mixed Layer. Proc., Aha Huliko'a, Hawaiian Winter Workshop,* University of Hawaii at Manoa, P. Müller and D. Henderson, Eds., 67–94.

Moum, J. N., D. R. Caldwell and C. A. Paulson, 1989: Mixing in the equatorial surface layer and thermocline. *J. Geophys. Res.,* **94,** 2005–2021.

Peters, H., M. C. Gregg and J. M. Toole, 1989: Meridional variability of turbulence through the equatorial undercurrent. *J. Geophys. Res.,* **94,** 18 003–18 009.

Stevenson, J. W., 1982: Computation of heat and momentum fluxes at the sea surface during the Hawaii to Tahiti Shuttle experiment. Hawaii Inst. Geophys. Rep. No. HIG-82-4, 42 pp.

——, and P. P. Niiler, 1983: Upper ocean heat budget during the Hawaii-to-Tahiti Shuttle experiment. *J. Phys. Oceanogr.,* **13,** 1894–1907.

Williams, R. T., 1981: Hawaii-Tahiti Shuttle experiment. CTD data report. 15 Volumes, Scripps Institution of Oceanography, University of California, San Diego.

Wyrtki, K., 1964: The thermal structure of the eastern Pacific Ocean. *Dtsch. Hydrogr. Ze.,* Suppl. **A8,** 6–84.

——, and B. Kilonsky, 1984: Mean water and current structure during the Hawaii-to-Tahiti Shuttle Experiment. *J. Phys. Oceanogr.,* **14,** 242–254.

——, E. Firing, D. Halpern, R. Knox, G. J. McNally, W. C. Patzert, E. D. Stroup, B. A. Taft and R. Williams, 1981: The Hawaii-to-Tahiti Shuttle experiment. *Science,* **211,** 22–28.